Rational Design of Fluorescent Bioimaging Probes by Controlling the Aggregation Behavior of Squaraines: A Special Effect of Ionic Liquid Pendants

ARTICLE *in* CHEMISTRY - A EUROPEAN JOURNAL · MAY 2010

Impact Factor: 5.73 · DOI: 10.1002/chem.200903492 · Source: PubMed

6 AUTHORS, INCLUDING:

Afu Fu
Nanyang Technological University
21 PUBLICATIONS **332** CITATIONS
SEE PROFILE

Ge Gao
Sichuan University
45 PUBLICATIONS **960** CITATIONS
SEE PROFILE

DOI: 10.1002/chem.200903492

Rational Design of Fluorescent Bioimaging Probes by Controlling the Aggregation Behavior of Squaraines: A Special Effect of Ionic Liquid Pendants

Wenhai Wang,[a] Afu Fu,[b] Jingbo Lan,[a] Ge Gao,[a] Jingsong You,*[a, b] and Lijuan Chen*[b]

Abstract: We herein present an effective strategy to create water-soluble fluorescent bioimaging dyes by introducing the imidazolium-based ionic liquid (IL) pendants into a fluorescent skeleton. A new type of water-soluble imidazolium-anchored squaraine dye was synthesized accordingly. The relationship between the aggregate of squaraines and their fluorescent cell imaging application was elucidated in detail. Firstly, the aggregation behavior of squaraines in water solutions could be suppressed by varying the alkyl chain attached to the imidazolium unit. Secondly, the capability of cellular uptake and staining of dyes was also dramatically enhanced upon increasing the length of the paraffinic chain. These squaraine dyes displayed an excellent photostability that could permit real-time fluorescence bioimaging experiments to be monitored over a long time period with constant sample irradiation. Additionally, we designed for the first time an Fe^{II}-ion probe on the basis of an attack of the hydroxyl radical to the four-membered ring of squaraine. The results demonstrated that the imidazolium-anchored squaraines could perform "naked-eye" detection of the Fe^{2+} ion over a wide range of other interfering metals in aqueous media. More surprisingly, this process showed a fluorescence "turn-off" and "-on" response through the regeneration of squaraines in cells.

Keywords: aggregation · bioimaging agents · sensors · ionic liquids · squaraines

Introduction

Molecular bioimaging by using synthetic fluorescent probes is a rapidly developing technology that is expected to recognize and sense the presence of cellular analytes, such as metal cations, anions, and biomolecules, to early identify diseases and to accelerate the drug discovery process.[1] Of bioimaging agents, the red/near-IR (NIR) dyes in the 605–900 nm wavelength region are preferred in molecular imaging studies of living subjects because their spectral properties are generally independent from biological interferences, such as light scattering, autoabsorption, and autofluorescence of biomolecules.[2] Despite considerable effort, the availability of such bioimaging dyes is limited to a certain extent for a variety of reasons, including water solubility, photostability, toxicity, etc.[1,2] Accordingly, the development of new fluorescent bioimaging probes still remains an attractive and promising goal.

Squaraines are a particularly promising class of organic dyes that exhibit unique photophysical properties, namely, a sharp and intense absorption band in the red to NIR region. In recent years, squaraine dyes have been extensively used in photoconductivity, optical data storage, solar cell, low-gap polymers, nonlinear optics, photosensitizers for photodynamic therapy (PDT),[3,4] and chemosensors.[5] Despite advantageous optical properties for biological imaging, studies pertaining to squaraine dyes as a versatile fluorescent scaffold for constructing bioimaging probes are very few so far.[6] It is conceivable that a pronounced tendency to form

[a] W. Wang, Prof. Dr. J. Lan, Prof. Dr. G. Gao, Prof. Dr. J. You
Key Laboratory of Green Chemistry and
Technology of Ministry of Education
College of Chemistry and State Key Laboratory of Biotherapy
West China Medical School, Sichuan University
29 Wangjiang Road, Chengdu 610064 (PR China)
Fax: (+86) 28-85412203
E-mail: jsyou@scu.edu.cn

[b] A. Fu, Prof. Dr. J. You, Prof. Dr. L. Chen
State Key Laboratory of Biotherapy, West China Hospital
West China Medical School, Sichuan University
Keyuan Road 4, Gaopeng Street, Chengdu 610041 (PR China)
Fax: (+86) 28-85164060
E-mail: lijuan17@hotmail.com

Supporting information for this article is available on the WWW under http://dx.doi.org/10.1002/chem.200903492.

H- and J-type aggregates induced fluorescent self-quenching in aqueous media has seriously hindered the achievement of this goal.[7] Thus, controlling the aggregation behavior of this type of chromophore in water solutions is an absolutely critical issue, and still remains a major challenge. To solve this problem, the concept of encapsulating squaraine dyes has been employed to provide substantial steric protection of the squaraine chromophore and thus inhibit aggregation.[6a,b] Quite recently, the aggregation behavior of π-extended squaraines has been uncovered to be diminished upon the addition of Cremophor EL (CrEL, polyethoxylated castor oil), frequently used in vivo as a nonionic solubilizer and emulsifier in the delivery of poorly water-soluble drugs.[6c]

The imidazolium salts, a well-known kind of cationic N-heteroaromatic compound, have especially attracted attention in the fields of ionic liquid, host-guest, and material chemistry in the past decade. Task-specific ionic liquids (TSILs) can provide a facile and promising route to multifunctional compounds.[8,9] Drawing from our recent experiences in TSILs,[10] we herein present a strategy to create water-soluble fluorescent bioimaging dyes by introducing the imidazolium-based ionic liquid pendants into a squaraine skeleton. We found that these new types of water-soluble imidazolium-anchored dyes could be converted into bright fluorescent bioimaging probes by controlling their aggregation behavior in aqueous media depending on the length of the alkyl tail (Scheme 1). The introduction of imidazolium-based ionic liquid termini would fulfill the following objectives: Firstly, the presence of the imidazolium pendants can greatly improve the solubility of squaraine dyes in water. Secondly, the imidazolium cation would not only be a driving force for cellular entry, but also facilitate a decreased tendency for aggregation due to electrostatic repulsion between the positive charges. Thirdly, the introduction of an imidazolium unit can render them amphiphilic and thereby enhance their cell permeability and eventually their use as bioimaging probes. More importantly, the amphipathicity and aggregation behavior of squaraine dyes may be easily controlled owing to convenient modification of the length of the paraffinic chain attached to the imidazolium unit.

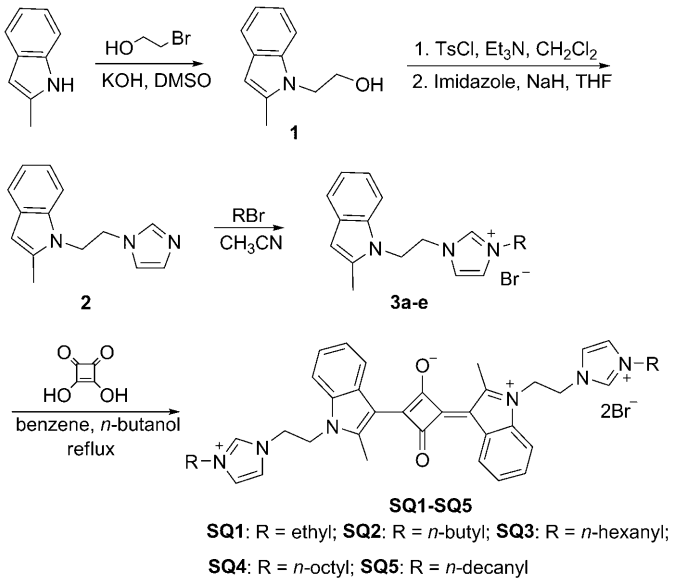

Scheme 1. Synthetic route of squaraines **SQ1**–**SQ5**. TsCl = 4-toluenesulfonyl chloride.

Results and Discussion

Synthesis of squaraines: Scheme 1 shows the synthetic strategy used to obtain imidazolium-anchored squaraines. The synthesis is a straightforward process starting from 2-methyl-1*H*-indole. The coupling of 2-methyl-1*H*-indole with 2-bromoethanol afforded 1-(2-hydroxylethyl)-2-methyl-1*H*-indole (**1**), followed by sequential treatment with tosyl chloride and imidazole. The resulting 1-[2-(1*H*-imidazol-1-yl)ethyl]-2-methyl-1*H*-indole (**2**) then reacted with *n*-bromoalkanes to give 1-[2-(3-alkylimidazolium)ethyl]-2-methyl-1*H*-indole bromides (**3**). Five representative squaraine dyes **SQ1**–**SQ5** were prepared by the condensation of **3** with squaric acid in *n*-butanol/benzene 1:1 v/v under reflux. Notably, as 1*H*-indole was used as the starting material, the reaction of the alkylimidazolium-based indole bromide and squaric acid could not give rise to the desired squaraines. In contrast to the vast majority of the known bioimaging dyes, the imidazolium-anchored squaraines, especially for **SQ1**–**SQ4**, showed a good solubility in water, which suggested that their aqueous solutions could be employed directly for cell imaging without the use of solubilizing agents, such as surfactants or organic solvents (e.g., ethanol, DMSO).

Photophysical properties and aggregation behavior of squaraines: To gain an insight into the correlation of aggregation behavior with molecular structure, the UV/Vis spectra of **SQ1**–**SQ5** were studied both in organic solvents and aqueous media. For example, in acetonitrile, all of the dyes **SQ1**–**SQ5** exhibited a characteristic sharp and intense absorption band centered around 576 nm that is indicative of the presence of monomeric, that is, nonaggregated, squaraine chromophores only (Figure 1A). In contrast, the aggregation behavior of dyes was clearly observed in cell culture fluids. As shown in Figure 1B, the two absorbance bands at approximately 540 and 574 nm could be assigned to the aggregated and monomeric forms in D-Hank's balanced salt solution (D-HBSS; for bands in Dublecco's minimum essential medium (DMEM), see Figure S1 in the Supporting Information). The hypsochromic shifts of the absorption maxima indicated the formation of H-type aggregates. Surprisingly, we found that increasing the length of the paraffinic chain led to a gradual decrease in the intensities of the aggregate bands at approximately 540 nm with a simultaneous increase in the intensities of the bands at approximately 574 nm. As the alkyl tail became the decanyl chain in **SQ5**, the aggregate band nearly disappeared. From the data presented in Figure 1C, the fluorescence intensities would be enhanced by

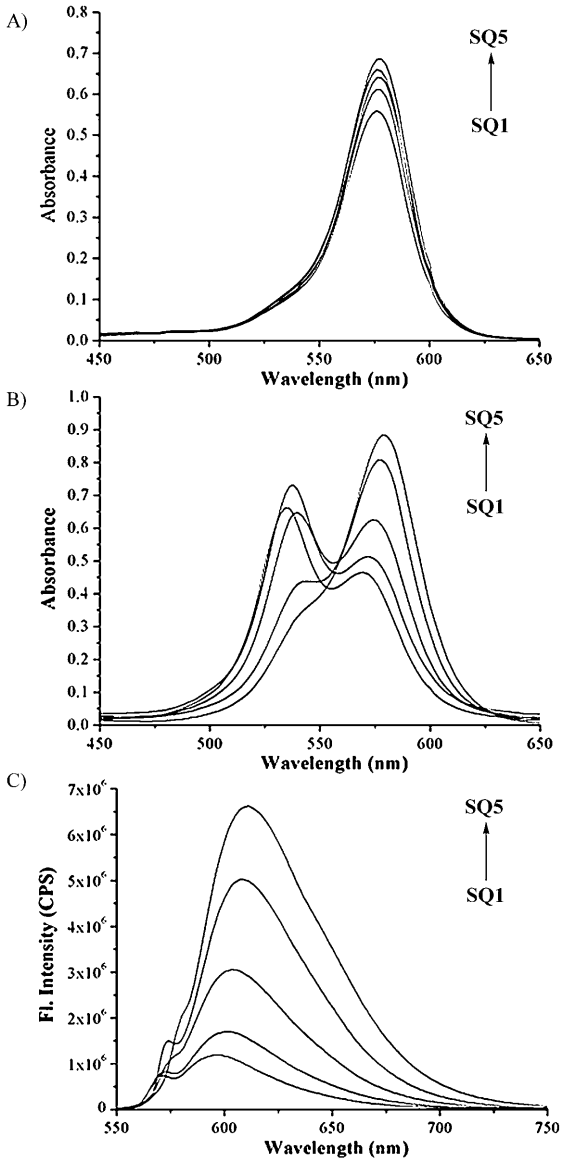

Figure 1. A) Absorption spectra of **SQ1**–**SQ5** (5 μM) recorded in CH_3CN at 25 °C. B) Absorption spectra and C) fluorescence spectra (slits = 5.0 nm) of **SQ1**–**SQ5** (10 μM) in D-HBSS at 37 °C.

lengthening the paraffinic chain (for the fluorescent quantum yields, see Table S1 in the Supporting Information). Herein, we draw a conclusion that the aggregation behavior of imidazolium-anchored squaraines in aqueous media could be suppressed by varying the length of the hydrocarbon chain, which would open the door to their applications in live cell imaging and single-molecule studies. More interestingly, reported studies demonstrated that amphiphilic squaraine dyes with quaternary ammonium head groups located at the end of molecules exhibited the increasing tendency towards aggregation as the length of the alkyl chain increased.[7b]

In addition, the absorption spectra of dyes **SQ1**–**SQ3** in acetonitrile/water mixtures of different compositions showed significant changes. To take **SQ2** as an example, a gradual increase in the intensities of the bands at 574 nm was detected as the percentage of acetonitrile in the solution was increased (Figure 2A). Similar to solvent composition,

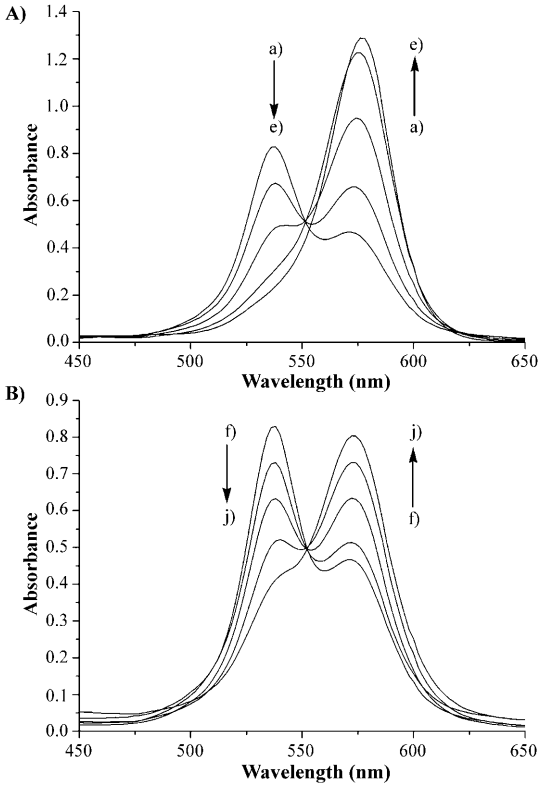

Figure 2. A) Absorption spectra of **SQ2** (10 μM) recorded in D-HBSS/CH_3CN with an increasing fraction of CH_3CN (v/v) at 25 °C: a) 1:0, b) 20:1, c) 9:1, d) 4:1, and e) 0:1. B) Absorption spectra of **SQ2** (10 μM) recorded in D-HBSS with increasing temperature from 25 to 70 °C: f) 25, g) 37, h) 50, i) 60, and j) 70 °C.

temperature also had a marked effect on the aggregation of dyes in D-HBSS. For example, as the temperature was increased from 25 to 70 °C, the aggregate band of **SQ2** almost disappeared completely (Figure 2B).

TEM analyses were further conducted to investigate the aggregation behavior of squaraines in D-HBSS. As illustrated in Figure 3, TEM images of **SQ2**, **SQ4**, and **SQ5**, dip cast on a polyvinyl formal coated copper grid revealed the appearance of spherical particles. To our surprise, the sizes of the particles observed did become quite different. The diameters of the particles of **SQ2**, **SQ4**, and **SQ5** estimated were 0.3–2 μm and approximately 25 and 20 nm, respectively, which disclosed that the aggregate formation was remarkable on **SQ2** relative to those on **SQ4** and **SQ5**. In combination with the UV/Vis spectrum studies, these results were indicative of the different driving forces involved in the aggregation process among **SQ2**, **SQ4**, and **SQ5**. The self-aggregation mode of dyes might be governed by a competition between π-stacking interactions of the chromophores and hydrophilic–hydrophobic interactions arising from the imi-

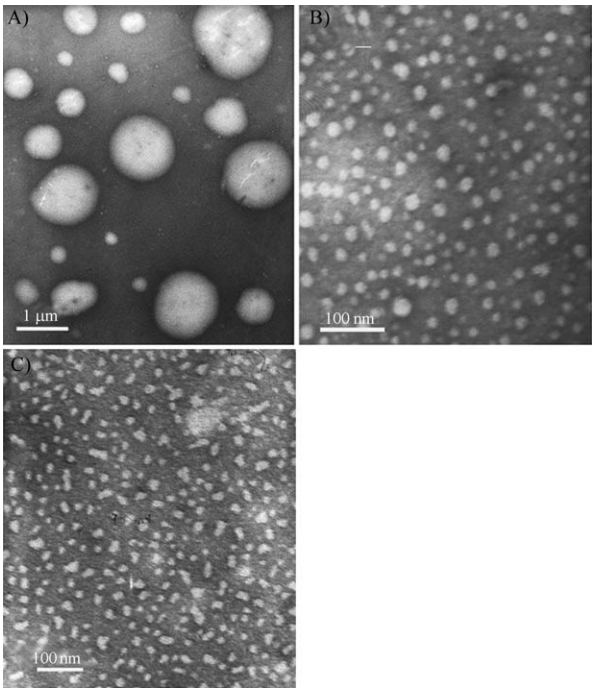

Figure 3. TEM images (stained with sodium phosphotungstate) of self-assembled structures of A) **SQ2**, B) **SQ4**, and C) **SQ5** (20 μM) in D-HBSS.

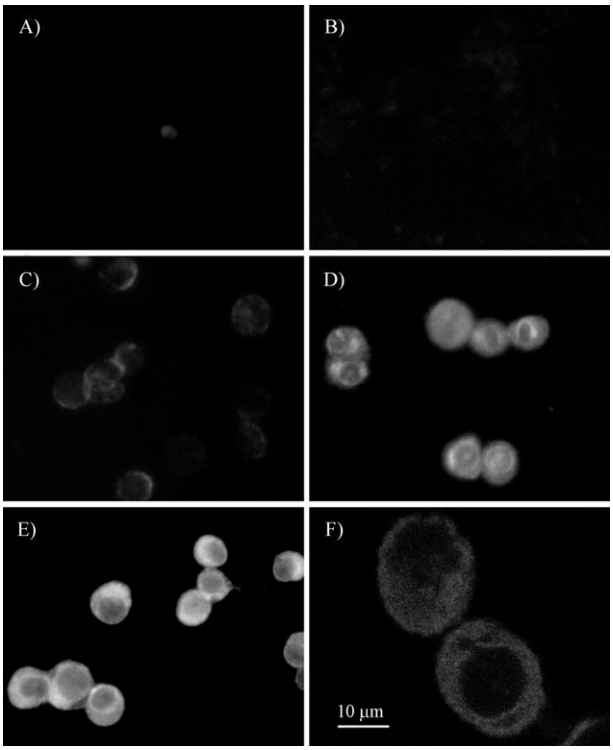

Figure 4. Fluorescence microscopy images (original magnification 200×) of live LL/2 cells treated with squaraines (20 μM) in D-HBSS for 15 min. A) **SQ1**, B) **SQ2**, C) **SQ3**, D) **SQ4**, E) **SQ5**, and F) CLSM images of LL/2 cells treated with **SQ4** in D-HBSS (20 μM) for 15 min. For color picture, see Figures S2 and S6 in the Supporting Information.

dazolium units and the anchored alkyl tails, which was clearly dependent on the length of the paraffinic chain. In **SQ2**, the H-type aggregation behavior, attributed to face-to-face π-stacking interactions between the chromophores, could be seen as a main driving force in the formation of large particles. As the length of the hydrocarbon chain increases, however, the entropic disadvantage may reduce the stability of the H-type aggregation,[11] and the inner squaraine chromophores are difficult to get close enough to interact. In the case of **SQ4** and **SQ5**, the formation of particles was dominated by the hydrophobic effect, which suggested that the self-assembly might be primarily forced by the hydrophilic–hydrophobic interactions aforementioned.

Cell fluorescent imaging: To assess the cell imaging efficiency of the squaraines, Lewis lung carcinoma cells (LL/2) were incubated with their D-HBSS solutions (20 μM) for 15 min at 37 °C. Typical fluorescence images of live LL/2 cells are illustrated in Figure 4 (see also Figure S2 in the Supporting Information). As expected, the capability of cellular uptake and staining of dyes was enhanced dramatically upon increasing the length of paraffinic chain. We speculated that the lengthening tail could not only improve their luminescence abilities, but also facilitate the cellular uptake owing to the enhanced lipophilicity and the suitable sizes of particles formed. In fact, in the case of **SQ1** and **SQ2**, these two dyes were poorly internalized even following a longer incubation time with a higher concentration (40 μM for 1 h). In sharp contrast, bright fluorescence images were rapidly captured in the cells after treatment with **SQ4** and **SQ5**, respectively, which indicated that the dyes permeated well through the cell membrane. The similar cellular imaging results were obtained when **SQ1**–**SQ5** were incubated with human hepatocellular carcinoma cells (HepG2), human cervica carcinoma cells (HeLa), and human umbilical vein endothelial cells (HUVEC), respectively (see Figures S3, S4, and S5 in the Supporting Information). Subsequently, visualization of localization within live LL/2 and HeLa cells was determined by using a confocal laser scanning microscope (CLSM). As demonstrated in Figure 4F and Figures S6 and S7 in the Supporting Information (CLSM images treated with Hoechst 33258 (cell nuclei stained)), the squaraine **SQ4** preferentially accumulated in the cytoplasm, and especially around the perinuclear region. Further increasing the incubation time to 30 min did not change the subcellular localization of **SQ4** (20 μM).

To evaluate the cytotoxicity of the probes, **SQ4** was taken as an example to perform a MTT assay on HepG2 cells with dye concentrations from 5 to 20 μM. The cellular viability estimated was approximately 96% at 4 h after treatment with 20 μM of **SQ4** (see Figure S8 in the Supporting Information), exhibiting low toxicity to cultured cells. Of stringent prerequisites, photostability is primary for imaging molecules in live cells. The high photostability of dyes permits real-time fluorescence bioimaging experiments to be monitored over a long time with constant sample irradiation. In this context,

the sample of LL/2 cells stained with **SQ4** was irradiated continuously with the green channel ($\lambda = 540$ to 580 nm) from a fluorescence inverted microscope. As shown in Figure 5 and Movie 1 in the Supporting Information, the fluorescence intensity still remained strong even after one hour, which showed that **SQ4** had excellent photostability. To our knowledge, such a type of experiment with currently available NIR cyanine dyes are less exhibited owing to their rapid photobleaching. It's comparable with a recent example that showed that squaraine rotaxanes were highly resistant to photobleaching with 1080 s of the photobleaching half-life.[6a] These results suggested that **SQ4** could serve as a fluorescent probe for live cell imaging.

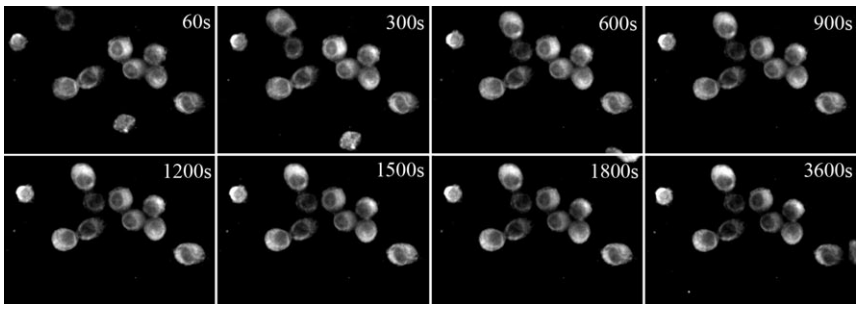

Figure 5. LL/2 cells stained with **SQ4** (20 μM) were imaged in D-HBSS with continuous irradiation for 60 min by a fluorescence inverted microscope.

Fe^{2+}-selective probe: Both Fe^{2+} and Fe^{3+} play vital roles in many biological processes, and deficiencies or excesses of these ions can lead to various diseases or promote excessive free-radical formation.[12] Detection and analysis of iron in vivo represents an important healthcare necessity. Although a number of fluorescent sensors have been devoted to recognizing Fe^{3+},[12a,13] there are relatively few reports on Fe^{2+} ones.[14] Considering the easily oxidized character of Fe^{2+}, utilizing a simple, rapid, and specific oxidative reaction to distinguish between Fe^{2+} and other metal ions would be an attractive and promising strategy to design an Fe^{2+}-selective probe. It is well known that H_2O_2 is converted into hydroxyl and a hydroxyl radical in the Fenton reaction in the coexistence of Fe^{2+}. On the other hand, squaraines involve multiple possible resonance structures, such as doubly cross-linked polymethine-like π-system (Scheme 2a), donor-acceptor-donor (b), and biradicaloid form (c),[15] and their central four-membered ring may be subjected to nucleophilic or radical attack at the equivalent 2- and 4-positions. Such a types of transformation in combination with the Fenton Reaction should be an ideal candidate to elucidate our tactics (Scheme 3). As expected, we herein discovered that the imidazolium-anchored squaraines could perform "naked-eye" detection of Fe^{2+} ion over a wide range of other interfering metals in aqueous media, as far as we know, which constitutes the first squaraine-based sensors dependent on the hydroxyl radical reaction.

As displayed in Figure S9 (see the Supporting Information), no color variation occurred upon individual addition of Fe^{2+} or H_2O_2 into a 4-(2-hydroxyethyl)-1-piperazineethanesulfonic acid (HEPES, 10 mM, pH 7.2) buffer solution of **SQ4**, whereas a remarkable bleaching of **SQ4** was observed with concomitant fluorescence quenching and UV/Vis absorption disappearance in the presence of both of Fe^{2+} and H_2O_2 (Figure 6), which could be attributed to the hydroxyl radical rather than hydroxyl in the Fenton reaction. It could be proved easily as the addition of even a 40 equivalent molar amount of hydroxyl into a HEPES buffer solution of **SQ4** induced negligible absorbance and fluorescence changes. On the basis of the previously reported squaraine-based sensors for the cyanide anion and thiol-containing biomolecules,[5c,d,i] we rationalized that the proposed action mechanism of the

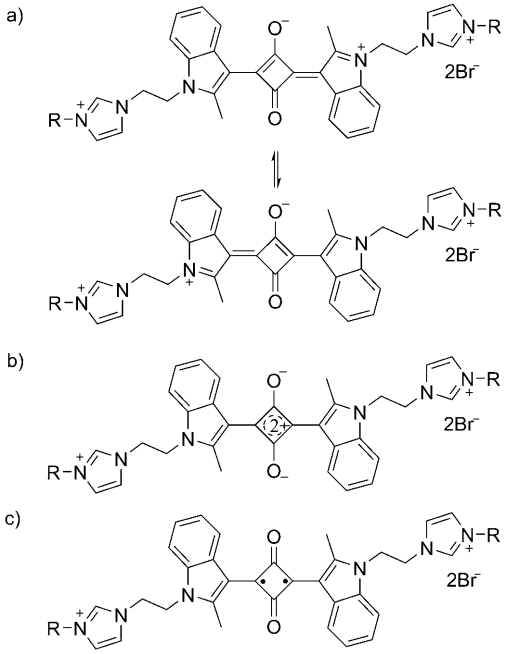

Scheme 2. The possible resonance structures of squaraine.

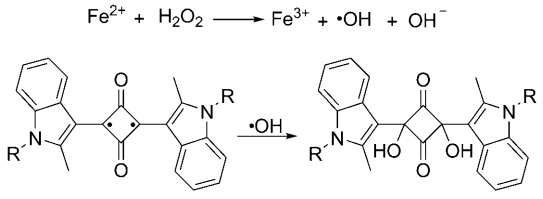

Scheme 3. A strategy to design an Fe^{2+} probe based on squaraine and the Fenton reaction.

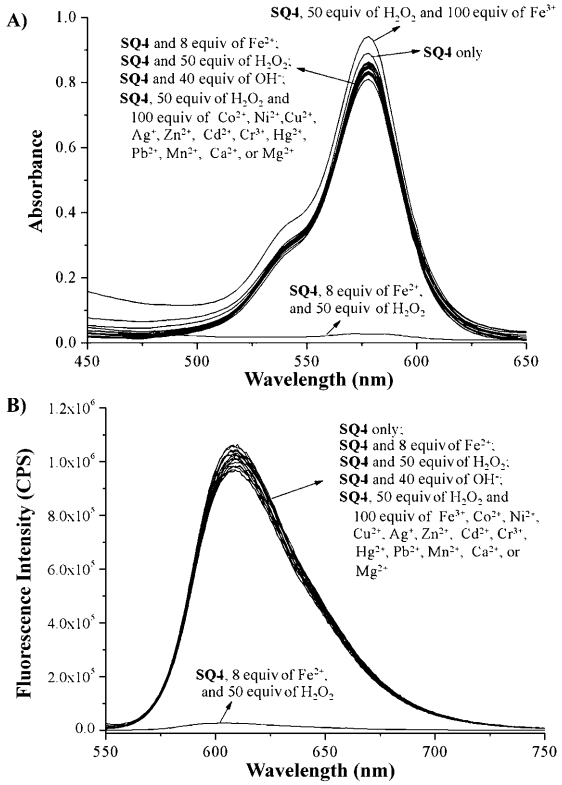

Figure 6. Absorbance response (A), and fluorescence response (B) of **SQ4** (10 μM) in HEPES buffer solutions (0.01 M, pH 7.2) containing H_2O_2 toward various metal ions at 25 °C (excitation wavelength = 535 nm, slit = 4.0 nm).

Fe^{2+} probe might involve an attack of the hydroxyl radical to the four-membered ring of squaraine (see Scheme 3 and Scheme S1 in the Supporting Information), which was further confirmed by the electrospray ionization (ESI) mass spectrum analysis. The ESI spectra of the corresponding adduct of the hydroxyl radical and **SQ4** (in a 2:1 ratio) showed the peaks at *m*/*z*: 787.4880 and 394.2486 (see Figure S11 in the Supporting Information). To further investigate the reaction mechanism between squaraine and hydroxyl radical, the squaraine **SQ6** lacking the ionic liquid pendants was synthesized. The ESI spectrum gave rise to the two peaks that were in accordance with the corresponding adducts of the hydroxyl radical and **SQ6** in 2:1 and 1:1 ratios (see Scheme S2 and Figure S12 in the Supporting Information).

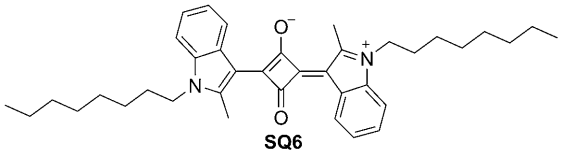

SQ6

Competition studies with other environmentally important metal ions, such as Fe^{3+}, Ag^+, Ca^{2+}, Zn^{2+}, Pb^{2+}, Cd^{2+}, Cu^{2+}, Co^{2+}, Hg^{2+}, Mn^{2+}, Ni^{2+}, Cr^{3+}, and Mg^{2+} underscored the selective response of **SQ4**. In a typical experiment, even upon the addition of 100 equivalents of metal ion into a solution of **SQ4**, the potential competitor nearly remained silent with respect to absorption, excitation, and color variation (see Figure 6 and Scheme S10 in the Supporting Information). Taken together, these data clearly established that **SQ4** could act as a selective probe for Fe^{2+}.

Fluorescent sensors that can selectively monitor specific metal ions in live cells have been indispensable tools for the understanding of biological phenomena. To determine whether **SQ4** could be used as an Fe^{2+} probe in live cells, LL/2 cells were first incubated with **SQ4** (10 μM) for 15 min, followed by the addition of 10 equivalents of Fe^{2+} for 1 min, and then the addition of 50–100 equivalents of H_2O_2. Figure 7 (for color picture, see Figure S13 in the Supporting Information) and Movie 2 (see the Supporting Information) showed the time-dependent fluorescence-microscopy images of live LL/2 cells. One might see that a clear red intracellular fluorescence disappeared upon the addition of both $FeCl_2$ and H_2O_2. More surprisingly, the cells could light up renewably in 20 min after a fluorescence "turn-off" response, and strong red fluorescence would be retained for a long time. Subsequently, we further investigated HeLa cells in the presence of 50 equivalents of H_2O_2, and a similar result was obtained (see Figure S14 and Movie 3 in the Supporting Information). This interesting phenomenon appeared to have never been observed before. Although the detailed mechanism was not well understood in this stage, we speculated that the dehydroxylase was responsible for eliminating the hydroxyl to regenerate the corresponding

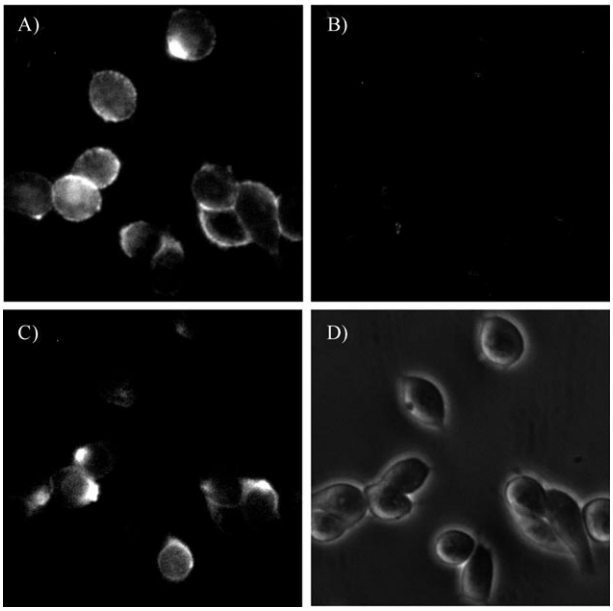

Figure 7. LL/2 cells were incubated with **SQ4** (10 μM) at 37 °C. Fluorescence image before (A) and after (B) addition of both of Fe^{2+} (10 equiv) and H_2O_2 (100 equiv). C) The renewed fluorescence image after its disappearance in B. D) Brightfield image of the cells. For color picture, see Figure S13 in the Supporting information.

fluorescent squaraine **SQ4**. Notably, the Hg^{2+}-ion triggered regeneration of squaraines was recently carried out by reversible bleaching reactions upon nucleophilic attack of propanethiol, allowing for straightforward "naked-eye" monitoring of the Hg^{2+}-ion detection process.[16]

Conclusion

We have successfully introduced the imidazolium-based ionic liquid pendants into squaraine to construct a new class of water-soluble bright fluorescent bioimaging dyes with marked photostability. The aggregation tendency in aqueous media and the capability of cellular uptake and staining of squaraines can be efficiently controlled by adjustment of the length of the alkyl chain attached to the imidazolium moiety. We believe that our strategy is generally applicable and may easily be extended to other bioimaging dyes. This class of water-soluble, highly photostable, and low toxic squaraines can be employed as a Fe^{2+}-selective probe. This process has demonstrated a fluorescence "turn-off" and "-on" response through the regeneration of squaraines in cells. Such a sensor would become valuable in revealing the roles of Fe^{2+} in biological systems under either in vitro or in vivo conditions. On the other hand, the overproduction of reactive oxygen species (ROS) in living organisms is implicated in the development of many severe diseases, such as inflammatory diseases, neurodegenerative diseases, and diabetes, etc.[17] Considering that this class of Fe^{2+} sensors are dependent on the reaction of squaraine and hydroxyl radical, we anticipate that the imidazolium-anchored squaraines will potentially serve as a fluorescence probe for hydroxyl-radical-related biological studies.

Experimental Section

General remarks: ^{1}H and ^{13}C NMR spectra were recorded on a Bruker AV-400 (^{1}H: 400, ^{13}C: 100 MHz) or a Varian INOVA-400 (^{1}H: 400, ^{13}C: 100 MHz). The ^{1}H NMR spectroscopic chemical shifts were measured relative to TMS ($\delta = 0.00$ ppm) for $CDCl_3$ or relative to [D_6]DMSO and D_2O as indicated. The ^{13}C NMR chemical shifts were given relative to [D_6]DMSO and $CDCl_3$ as indicated. LRMS were obtained on a Waters Quattro Premier XE Mass Spectrometer. HRMS were recorded on a Waters-TOF Premier Mass Spectrometer by positive ESI-Q-TOF. Absorption spectra were obtained on a HITACHI U-2910 spectrometer. Fluorescence-emission spectra were obtained by using a FluoroMax-4 (JONIN-YVON, HORIBA) spectrofluorophotometer. TEM studies were carried out on a HITACHI H-600IV, operating at 75 kV. Melting points of compounds were recorded on a XT-4 thermal apparatus and are uncorrected. Unless otherwise noted, materials were obtained from commercial suppliers and were used without further purification. *n*-Butanol was dried by heating at reflux over sodium and distilled prior to use. Benzene was treated firstly by shaking with concentrated H_2SO_4 until free form thiophene was formed, and then with water, dilute NaOH and water again. This mixture was then dried with sodium and distilled prior to use. All syntheses and manipulations were carried out under a dry N_2 atmosphere. The solutions of metal ions were prepared from $FeCl_2{\cdot}4H_2O$, $FeCl_3{\cdot}6H_2O$, $CoCl_2{\cdot}6H_2O$, $NiCl_2{\cdot}6H_2O$, $CdCl_2{\cdot}2.5H_2O$, $CaCl_2$, $CuCl_2{\cdot}2H_2O$, $CrCl_3{\cdot}6H_2O$, $ZnCl_2$, $MgCl_2$, $AgNO_3$, $Pb(OAc)_2{\cdot}3H_2O$, and $Hg(OAc)_2$, respectively, and were dissolved in redistilled water. The squaraine **SQ6** was synthesized according to the literature.[18]

1-(2-Hydroxylethyl)-2-methyl-1*H*-indole (1): 2-Methyl-1*H*-indole (5.25 g, 40 mmol) was added to a suspension of potassium hydroxide (8.98 g, 160 mmol) in DMSO (40 mL) under an atmosphere of nitrogen. After the mixture had been stirred for 1 h, 2-bromoethanol (6.25 g, 50 mmol) was added with external cooling (ice bath). The resulting mixture was then stirred for another 12 h. Water (40 mL) was added and the mixture was extracted with dichloromethane (3×40 mL). The combined organic layers were dried over anhydrous Na_2SO_4 and concentrated under reduced pressure. The crude material was purified by column chromatography on silica gel eluting with petroleum ether/EtOAc (4:1, v/v) to afford the desired product as a yellow solid (3.78 g, 54%). M.p. 92–94°C; ^{1}H NMR (400 MHz, $CDCl_3$): $\delta = 2.44$ (s, 3H), 3.87 (t, $J = 5.6$ Hz, 2H), 4.20 (t, $J = 5.6$ Hz, 2H), 7.05 (t, $J = 7.2$ Hz, 1H), 7.11 (m, 1H), 7.27 (d, $J = 8.0$ Hz, 1H), 7.50 ppm (d, $J = 8.0$ Hz, 1H); ^{13}C NMR (100 MHz, $CDCl_3$): $\delta = 11.9$, 44.2, 60.5, 99.1, 108.1, 118.5, 118.8, 119.6, 127.1, 135.8, 136.1 ppm; MS (ESI): *m*/*z*: calcd for $C_{11}H_{14}NO$: 176.1 $[M+H]^+$; found: 176.1.

1-[2-(1*H*-Imidazol-1-yl)ethyl]-2-methyl-1*H*-indole (2): Tosyl chloride (4.5 g, 23.8 mmol) in dicloromethane (20 mL) was added dropwise to a solution of 1-(2-hydroxylethyl)-2-methyl-1*H*-indole (**1**) (3.8 g, 21.7 mmol) and triethylamine (15 mL) in dicloromethane (20 mL). The solution was then stirred for 6 h at room temperature. After the accumulated triethylamine hydrochloride salt had been removed by filtration, the filtrate was evaporated to dryness. The residue was washed by hot petroleum ether and the yellow solid was used directly in the next reaction.

Sodium hydride (60% in mineral oil, 0.876 g, 21.9 mmol) was added to a solution of imidazole (1.35 g, 19.9 mmol) in THF (20 mL). After the solution had been stirred for 30 min at 40°C, a THF (30 mL) solution of the yellow solid obtained in the previous step (5.95 g, 18.1 mmol) was added dropwise over 30 min. The resulting mixture was then stirred vigorously for 12 h at 75°C. Subsequently, the solid was removed by filtration and the filtrate was evaporated to dryness. The residue was purified by flash column chromatography on silica gel eluting with CH_2Cl_2/CH_3OH (16:1, v/v) to give **2** as a light-yellow powder (3.51 g, 72%). M.p. 91–93°C; ^{1}H NMR (400 MHz, $CDCl_3$): $\delta = 1.90$ (s, 3H), 4.26–4.29 (m, 2H), 4.31–4.34 (m, 2H), 6.19 (s, 1H), 6.50–6.51 (m, 1H), 6.99 (s, 1H), 7.09–7.14 (m, 2H), 7.16–7.17 (m, 2H), 7.53 ppm (d, $J = 7.6$ Hz, 1H); ^{13}C NMR (100 MHz, $CDCl_3$): $\delta = 11.9$, 44.3, 46.1, 100.8, 108.4, 119.3, 120.0, 120.2, 121.0, 128.6, 129.8, 135.9, 136.8, 137.1 ppm; MS (ESI): *m*/*z*: calcd for $C_{14}H_{16}N_3$: 226.1 $[M+H]^+$; found: 226.1.

General procedure for the synthesis of 3a–e: *n*-Bromoalkane (1 mL) was added to a solution of **2** (0.68 g, 3 mmol) in CH_3CN (1 mL). The solution was then stirred vigorously for 12 h at 75°C (40°C for **3a**). The desired product was acquired as a light-yellow solid by column chromatography on silica gel eluting with CH_2Cl_2/CH_3OH (20:1, v/v).

1-[2-(3-Ethylimidazolium)ethyl]-2-methyl-1*H*-indole bromide (3a): Yield: 0.89 g, 89%; m.p. 150–153°C; ^{1}H NMR (400 MHz, D_2O): $\delta = 1.16$ (t, $J = 7.2$ Hz, 3H), 2.32 (s, 3H), 3.88 (q, $J = 7.2$ Hz, 2H), 4.62 (s, 4H), 6.44 (s, 1H), 7.06–7.08 (m, 1H), 7.14–7.16 (m, 2H), 7.32 (d, $J = 1.6$ Hz, 1H), 7.36 (d, $J = 1.6$ Hz, 1H), 7.60–7.63 (m, 1H), 7.85 ppm (s, 1H); ^{13}C NMR (100 MHz, [D_6]DMSO): $\delta = 12.7$, 15.6, 43.0, 44.5, 49.0, 101.1, 109.0, 119.7, 119.8, 120.7, 122.5, 123.5, 127.9, 136.5, 136.9, 137.0 ppm; MS (ESI): *m*/*z*: calcd for $C_{16}H_{21}N_3$: 255.2 $[M-Br+H]^+$; found: 255.0.

1-[2-(3-Butylimidazolium)ethyl]-2-methyl-1*H*-indole bromide (3b): Hygroscopic solid; yield: 0.99 g, 92%; ^{1}H NMR (400 MHz, $CDCl_3$): $\delta = 0.91$ (t, $J = 7.2$ Hz, 3H), 1.19–1.29 (m, 2H), 1.59–1.67 (m, 2H), 2.32 (s, 3H), 3.98 (t, $J = 7.6$ Hz, 2H), 4.67 (t, $J = 5.6$ Hz, 2H), 4.91 (t, $J = 5.6$ Hz, 2H), 6.25 (br s, 1H), 6.83 (s, 1H), 6.96 (s, 1H), 7.01–7.08 (m, 3H), 7.44–7.48 (m, 1H), 9.71 ppm (s, 1H); ^{13}C NMR (100 MHz, $CDCl_3$): $\delta = 13.1$, 13.5, 19.4, 32.0, 43.2, 49.3, 49.9, 101.8, 108.3, 120.1, 121.2, 121.8, 123.4, 127.9, 136.2, 136.4, 136.7 ppm; MS (ESI): *m*/*z*: calcd for $C_{18}H_{24}N_3$: 282.2 $[M-Br]^+$; found: 282.1.

1-[2-(3-Hexanylimidazolium)ethyl]-2-methyl-1*H*-indole bromide (3c): Yield: 1.08 g, 93%; m.p. 92–94°C; ^{1}H NMR (400 MHz, D_2O): $\delta = 0.91$ (t, $J = 7.2$ Hz, 3H), 1.04–1.12 (m, 2H), 1.22–1.37 (m, 4H), 1.41–1.48 (m, 2H), 2.30 (s, 3H), 3.83 (t, $J = 7.2$ Hz, 2H), 4.63 (s, 4H), 6.40 (s, 1H),

7.09–7.15 (m, 3H), 7.33 (m, 1H), 7.37–7.38 (m, 1H), 7.58–7.60 (m, 1H), 7.82 ppm (s, 1H); ^{13}C NMR (100 MHz, $CDCl_3$): δ = 12.9, 13.9, 22.3, 25.7, 29.9, 30.9, 43.0, 49.1, 50.0, 101.7, 108.2, 119.9, 121.1, 121.6, 123.3, 127.8, 136.0, 136.2, 136.5 ppm; MS (ESI): *m*/*z*: calcd for $C_{20}H_{28}Br_2N_3$: 468.1 $[M+Br]^-$; found: 468.0.

1-[2-(3-Octylimidazolium)ethyl]-2-methyl-1*H*-indole bromide (3d): Yield: 1.20 g, 96%; m.p. 102–105°C; ^{1}H NMR (400 MHz, D_2O): δ = 0.77–0.84 (m, 2H), 1.03–1.09 (m, 2H), 1.11–1.18 (m, 5H), 1.24–1.31 (m, 2H), 1.35–1.42 (m, 2H), 1.47–1.54 (m, 2H), 2.27 (s, 3H), 3.58 (t, *J* = 6.8 Hz, 2H), 4.59 (br s, 4H), 6.10 (s, 1H), 6.87 (t, *J* = 7.2 Hz, 1H), 6.93 (t, *J* = 8.0 Hz, 1H), 7.01–7.05 (m, 2H), 7.27 (d, *J* = 7.6 Hz, 1H), 7.42 ppm (s, 1H); ^{13}C NMR (100 MHz, $CDCl_3$): δ = 13.0, 14.2, 22.7, 26.2, 28.9, 29.8, 30.1, 31.8, 43.2, 49.3, 50.1, 101.8, 108.3, 120.1, 121.2, 121.6, 123.4, 127.9, 136.2, 136.4, 136.7 ppm; MS (ESI): *m*/*z*: calcd for $C_{22}H_{32}N_3$: 338.3; found: 338.3.

1-[2-(3-Decanylimidazolium)ethyl]-2-methyl-1*H*-indole bromide (3e): Yield: 1.27 g, 95%; m.p. 82–84°C; ^{1}H NMR (400 MHz, $CDCl_3$): δ = 0.87 (t, *J* = 6.8 Hz, 3H), 1.21–1.31 (m, 14H), 1.60–1.67 (m, 2H), 2.32 (s, 3H), 3.97 (t, *J* = 7.6 Hz, 2H), 4.67 (t, *J* = 5.6 Hz, 2H), 4.92 (t, *J* = 5.6 Hz, 2H), 6.26 (br s, 1H), 6.81 (s, 1H), 6.93 (s, 1H), 7.01–7.05 (m, 2H), 7.06–7.08 (m, 1H), 7.45–7.47 (m, 1H), 9.73 ppm (s, 1H); ^{13}C NMR (100 MHz, $CDCl_3$): δ = 12.9, 14.0, 22.6, 26.1, 28.8, 29.1, 29.2, 29.4, 30.0, 31.8, 43.0, 49.2, 50.0, 101.7, 108.2, 119.9, 121.1, 121.5, 123.3, 127.9, 136.0, 136.3, 136.6 ppm; HRMS: *m*/*z*: calcd for $C_{24}H_{36}N_3$: 366.2904 $[M-Br]^+$; found: 366.2901.

General preparation for the water-soluble imidazolium-anchored squaraines SQ1–SQ5: The imidazolium salt **3** (0.3 mmol) was added to a solution of squaric acid (3,4-dihydroxy-3-cyclobutene-1,2-dione; 17.1 mg, 0.15 mmol) in a mixture of anhydrous *n*-butanol (10 mL) and benzene (10 mL) in a flame-dried Schlenk test tube. The reaction mixture was then refluxed for 3 h. After being cooled and kept overnight at 0°C, the mixture was filtered and the solid was washed with isopropanol and hexane until the filtrate was almost colorless. The desired product was gained as a blue solid.

Squaraine ***SQ1***: Yield: 111.9 mg, 75%; m.p. 279–282°C; ^{1}H NMR (400 MHz, D_2O): δ = 1.07 (t, *J* = 7.2 Hz, 6H), 2.70 (s, 6H), 3.88–3.94 (m, 4H), 4.19 (s, 4H), 4.53 (s, 4H), 6.92 (d, *J* = 8.0 Hz, 2H), 7.30–7.33 (m, 5H), 7.37–7.41 (m, 3H), 8.06 (s, 2H), 8.56 ppm (d, *J* = 8.0 Hz, 2H); ^{13}C NMR (100 MHz, [D$_6$]DMSO): δ = 14.1, 15.7, 44.3, 44.7, 48.1, 110.4, 112.8, 122.8, 123.7, 124.5, 125.6, 126.6, 136.8, 139.0, 152.4, 188.3 ppm; HRMS: *m*/*z*: calcd for $C_{36}H_{39}Br_2N_6O_2Na$: 768.1399 $[M+Na+H]^+$; found: 768.1393; elemental analysis calcd (%) for $C_{36}H_{38}Br_2N_6O_2$: C 57.92, H 5.13, N 11.26; found: C 57.97, H 5.49, N 10.92.

Squaraine ***SQ2***: Yield: 72.1 mg, 60%; m.p. 256–258°C; ^{1}H NMR (400 MHz, D_2O): δ = 0.66 (t, *J* = 7.6 Hz, 6H), 0.82–0.92 (m, 4H), 1.35–1.42 (m, 4H), 2.68 (s, 6H), 3.87 (t, *J* = 7.2 Hz, 4H), 4.27 (s, 4H), 4.61 (s, 4H), 7.12 (d, *J* = 6.8 Hz, 2H), 7.40–7.47 (m, 6H), 7.50 (s, 2H), 7.94 (s, 2H), 8.63 ppm (d, *J* = 7.6 Hz, 2H); ^{13}C NMR (100 MHz, [D$_6$]DMSO): δ = 13.7, 14.1, 19.1, 31.9, 44.3, 48.2, 49.1, 110.5, 112.8, 123.2, 123.7, 123.8, 124.5, 125.6, 126.6, 137.0, 139.0, 152.3, 188.4 ppm; HRMS: *m*/*z*: calcd for $C_{40}H_{47}Br_2N_6O_2Na$: 824.2025 $[M+Na+H]^+$; found: 824.2029.

Squaraine ***SQ3***: Yield: 60.5 mg, 47%; m.p. 225–227°C; ^{1}H NMR (400 MHz, D_2O): δ = 0.60 (t, *J* = 6.8 Hz, 6H), 0.83–0.87 (m, 4H), 1.03–1.07 (m, 8H), 1.34–1.42 (m, 4H), 2.67 (s, 6H), 3.87 (t, *J* = 6.8 Hz, 4H), 4.21 (s, 4H), 4.60 (s, 4H), 7.08 (d, *J* = 7.2 Hz, 2H), 7.36–7.44 (m, 6H), 7.47 (s, 2H), 7.93 (s, 2H), 8.62 ppm (d, *J* = 7.2 Hz, 2H); ^{13}C NMR (100 MHz, [D$_6$]DMSO): δ = 14.1, 14.3, 22.3, 25.5, 29.9, 31.0, 44.3, 48.2, 49.3, 110.5, 112.8, 123.2, 123.6, 123.7, 124.5, 125.6, 126.6, 137.0, 139.0, 152.3, 179.4, 188.5 ppm; HRMS: *m*/*z*: calcd for $C_{44}H_{55}Br_2N_6O_2Na$: 880.2651 $[M+Na+H]^+$; found: 880.2643.

Squaraine ***SQ4***: Yield: 60.4 mg, 44%; m.p. 221–223°C; ^{1}H NMR (400 MHz, D_2O): δ = 0.64 (t, *J* = 7.2 Hz, 6H), 0.74–0.80 (m, 4H), 1.01–1.10 (m, 16H), 1.35–1.43 (m, 4H), 2.67 (s, 6H), 3.87 (t, *J* = 6.8 Hz, 4H), 4.20 (s, 4H), 4.59 (s, 4H), 7.07 (d, *J* = 6.4 Hz, 2H), 7.34–7.40 (m, 6H), 7.45 (s, 2H), 7.95 (s, 2H), 8.63 ppm (d, *J* = 7.6 Hz, 2H); ^{13}C NMR (100 MHz, [D$_6$]DMSO): δ = 14.1, 14.4, 22.5, 25.8, 28.8, 30.0, 31.6, 44.3, 48.2, 49.4, 110.5, 112.9, 123.2, 123.6, 123.7, 124.5, 125.7, 126.6, 137.0, 139.0, 152.3, 179.4, 188.6 ppm; HRMS: *m*/*z*: calcd for $C_{48}H_{61}N_6O_2$: 753.4856 $[M-2Br-H]^+$; found: 753.4855.

Squaraine ***SQ5***: Yield: 30.6 mg, 21%; m.p. 216–219°C; ^{1}H NMR (400 MHz, [D$_6$]DMSO): δ = 0.80 (t, *J* = 7.2 Hz, 6H), 1.03–1.04 (m, 4H), 1.17–1.23 (m, 24H), 1.48–1.56 (m, 4H), 3.17 (s, 6H), 4.00 (t, *J* = 7.2 Hz, 4H), 4.70–4.71 (m, 4H), 4.81–4.82 (m, 4H), 7.19–7.27 (m, 4H), 7.35 (d, *J* = 8.0 Hz, 2H), 7.75 (s, 2H), 7.83 (s, 2H), 8.98 (s, 2H), 9.05 ppm (d, 7.6 Hz, 2H); ^{13}C NMR (100 MHz, [D$_6$]DMSO): δ = 14.1, 14.4, 22.5, 25.8, 28.8, 29.1, 29.2, 29.4, 30.0, 31.7, 44.3, 48.2, 49.3, 110.5, 112.9, 123.2, 123.6, 124.4, 125.7, 126.6, 137.0, 139.0, 152.2, 179.3, 188.6 ppm; HRMS: *m*/*z*: calcd for $C_{52}H_{69}N_6O_2$: 809.5482 $[M-2Br-H]^+$; found: 809.5481; elemental analysis calcd (%) for $C_{52}H_{70}Br_2N_6O_2$: C 64.32, H 7.27, N 8.66; found: C 64.04, H 7.53, N 7.85.

Cell culture experiments: Lewis lung carcinoma cell line (LL/2), hepatocellular carcinoma cell line (HepG2), and human cervica carcinoma cell line (HeLa) were obtained from the American type culture collection (ATCC) and cultured in Dublecco's minimum essential medium (DMEM) containing 10% fetal bovine serum (FBS), L-glutamine (2 mM), penicillin (100 IU mL^{-1}), and streptomycin (100 μg mL^{-1}). All cells were incubated in an atmosphere of 5% CO_2 at 37°C.

Human umbilical vein endothelial cells (HUVEC) were isolated from human umbilical cord with collagenase and used at passage 2–3.[19] After dissociation, the cells were collected and cultured on gelatin-coated culture flasks in M199 medium with 20% FBS, bFGF (10 ng mL^{-1}), VEGF (2 ng mL^{-1}), penicillin (100 IU mL^{-1}), and streptomycin (100 μg mL^{-1}).

Fluorescence imaging of live cells: LL/2, HepG2, HeLa, or HUVEC cells (2×10^4/well) were plated into 24-well plates. After 24 h, cells were incubated with the squaraines **SQ1**–**SQ5** (20 μM) in a solution of D-HBSS (140 mM NaCl, 5.4 mM KCl, 1 mg mL^{-1} glucose, 0.44 mM KH_2PO_4, 0.37 mM $Na_2HPO_4\cdot12H_2O$, 4.2 mM $NaHCO_3$, pH 7.4) at 37°C for 15 min. Fluorescence images were then examined under a fluorescence inverted microscope (ZEISS Axiovert 200).

Confocal fluorescence imaging was performed with a Leica TCS SP2 confocal laser scanning microscope and a 60× oil-immersion objective lens. Excitation of **SQ4**-loaded cells at 543 nm was carried out with a HeNe laser. Excitation of Hoechst 33258-loaded cells at 405 nm was carried out with a semiconductor laser.

Intracellular fluorescence image for Fe^{2+}: LL/2 or HeLa cells (2×10^4/well) were plated into 24-well plates. After 24 h, cells were incubated with **SQ4** (10 μM) in a physiological saline for 15 min. After the cells were washed, $FeCl_2$ (10 equiv) was added. One minute later, H_2O_2 (50–100 equiv) was added. Subsequently, the fluorescence image was observed under a fluorescence inverted microscope. In a HEPES buffer solution, the similar imaging results were obtained.

Acknowledgements

This work was supported by grants from the National Natural Science Foundation of China (nos. 20602027, 20772086, and 20902063), National 863 of China (no. 2007AA021201), and PCSIRT (no. IRT0846). We also thank the Centre of Testing and Analysis, Sichuan University for TEM and NMR spectroscopic measurements. W.W. and A.F. contributed equally to this work.

[1] a) *Applied Fluorescence in Chemistry, Biology, and Medicine* (Eds.: W. Rettig, B. Strehmel, S. Schrader, H. Seifert), Springer, New York, **1999**; b) J. Zhang, R. E. Campbell, A. Y. Ting, R. Y. Tsien, *Nat. Rev. Mol. Cell Biol.* **2002**, *3*, 906–918; c) J. Rao, A. Dragulescu-Andrasi, H. Yao, *Curr. Opin. Biotechnol.* **2007**, *18*, 17–25; d) E. L. Que, D. W. Domaille, C. J. Chang, *Chem. Rev.* **2008**, *108*, 1517–1549; e) O. Thoumine, H. Ewers, M. Heine, L. Groc, R. Frischknecht, G. Giannone, C. Poujol, P. Legros, B. Lounis, L. Cognet, D. Choquet, *Chem. Rev.* **2008**, *108*, 1565–1587; f) M. S. T. Gonçalves, *Chem. Rev.* **2009**, *109*, 190–212.

[2] a) J. V. Frangioni, *Curr. Opin. Chem. Biol.* **2003**, *7*, 626–634; b) R. Weissleder, V. Ntziachristos, *Nat. Med.* **2003**, *9*, 123–128; c) R. Bandichhor, A. D. Petrescu, A. Vespa, A. B. Kier, F. Schroeder, K. Burgess, *J. Am. Chem. Soc.* **2006**, *128*, 10688–10689; d) K. Kiyose, H. Kojima, T. Nagano, *Chem. Asian J.* **2008**, *3*, 506–515; e) S. J. Lord, N. R. Conley, H.-lu D. Lee, R. Samuel, N. Liu, R. J. Twieg, W. E. Moerner, *J. Am. Chem. Soc.* **2008**, *130*, 9204–9205.

[3] For reviews, see: a) A. Ajayaghosh, *Acc. Chem. Res.* **2005**, *38*, 449–459; b) S. Sreejith, P. Carol, P. Chithra, A. Ajayaghosh, *J. Mater. Chem.* **2008**, *18*, 264–274; c) J. J. Gassensmith, J. M. Baumes, B. D. Smith, *Chem. Commun.* **2009**, 6329–6338; d) J. J. McEwen, K. J. Wallace, *Chem. Commun.* **2009**, 6339–6351.

[4] Selected recent examples, see: a) A. Ajayaghosh, J. Eldo, *Org. Lett.* **2001**, *3*, 2595–2598; b) Y. Geng, D. Katsis, S. W. Culligan, J. J. Ou, S. H. Chen, L. J. Rothberg, *Chem. Mater.* **2002**, *14*, 463–470; c) A. Ajayaghosh, *Chem. Soc. Rev.* **2003**, *32*, 181–191; d) J.-H. Yum, P. Walter, S. Huber, D. Rentsch, T. Geiger, F. Nüesch, F. de Angelis, M. Grätzel, M. K. Nazeeruddin, *J. Am. Chem. Soc.* **2007**, *129*, 10320–10321; e) L.-H. Liu, K. Nakatani, R. Pansu, J.-J. Vachon, P. Tauc, E. Ishow, *Adv. Mater.* **2007**, *19*, 433–436; f) E. C. P. Smits, S. Setayesh, T. D. Anthopoulos, M. Buechel, W. Nijssen, R. Coehoorn, P. W. M. Blom, B. de Boer, D. M. de Leeuw, *Adv. Mater.* **2007**, *19*, 734–738; g) H. Choi, S. Kim, S. O. Kang, J. Ko, M.-S. Kang, J. N. Clifford, A. Forneli, E. Palomares, M. K. Nazeeruddin, M. Grätzel, *Angew. Chem.* **2008**, *120*, 8383–8387; *Angew. Chem. Int. Ed.* **2008**, *47*, 8259–8263; h) S. A. Odom, S. Webster, L. A. Padilha, D. Peceli, H. Hu, G. Nootz, S.-J. Chung, S. Ohira, J. D. Matichak, O. V. Przhonska, A. D. Kachkovski, S. Barlow, J.-L. Brédas, H. L. Anderson, D. J. Hagan, E. W. Van Stryland, S. R. Marder, *J. Am. Chem. Soc.* **2009**, *131*, 7510–7511.

[5] Selected examples for chemosensors, see: a) C. R. Chenthamarakshan, A. Ajayaghosh, *Tetrahedron Lett.* **1998**, *39*, 1795–1798; b) C. R. Chenthamarakshan, J. Eldo, A. Ajayaghosh, *Macromolecules* **1999**, *32*, 5846–5851; c) J. V. Ros-Lis, R. Martínez-Máñez, J. Soto, *Chem. Commun.* **2002**, 2248–2249; d) J. V. Ros-Lis, B. García, D. Jiménez, R. Martínez-Máñez, F. Sancenón, J. Soto, J. Gonzalvo, M. C. Valldecabres, *J. Am. Chem. Soc.* **2004**, *126*, 4064–4065; e) E. Arunkumar, A. Ajayaghosh, J. Daub, *J. Am. Chem. Soc.* **2005**, *127*, 3156–3164; f) V. S. Jisha, K. T. Arun, M. Hariharan, D. Ramaiah, *J. Am. Chem. Soc.* **2006**, *128*, 6024–6025; g) P. T. Snee, R. C. Somers, G. Nair, J. P. Zimmer, M. G. Bawendi, D. G. Nocera, *J. Am. Chem. Soc.* **2006**, *128*, 13320–13321; h) Y. Suzuki, K. Yokoyama, *Angew. Chem.* **2007**, *119*, 4175–4177; *Angew. Chem. Int. Ed.* **2007**, *46*, 4097–4099; i) S. Sreejith, K. P. Divya, A. Ajayaghosh, *Angew. Chem.* **2008**, *120*, 8001–8005; *Angew. Chem. Int. Ed.* **2008**, *47*, 7883–7887.

[6] a) J. R. Johnson, N. Fu, E. Arunkumar, W. M. Leevy, S. T. Gammon, D. Piwnica-Worms, B. D. Smith, *Angew. Chem.* **2007**, *119*, 5624–5627; *Angew. Chem. Int. Ed.* **2007**, *46*, 5528–5531; b) J. J. Gassensmith, E. A. L. Barr, J. M. Baumes, K. M. DiVittorio, J. R. Johnson, B. C. Noll, B. D. Smith, *J. Am. Chem. Soc.* **2007**, *129*, 15054–15059; c) L. Beverina, M. Crippa, M. Landenna, R. Ruffo, P. Salice, F. Silvestri, S. Versari, A. Villa, L. Ciaffoni, E. Collini, C. Ferrante, S. Bradamante, C. M. Mari, R. Bozio, G. A. Pagani, *J. Am. Chem. Soc.* **2008**, *130*, 1894–1902.

[7] a) H. Chen, W. G. Herkstroeter, J. Perlstein, K.-Y. Law, D. G. Whitten, *J. Phys. Chem.* **1994**, *98*, 5138–5146; b) H. Chen, M. S. Farahat, K. Law, D. G. Whitten, *J. Am. Chem. Soc.* **1996**, *118*, 2584–2594; c) R. S. Stoll, N. Severin, J. P. Rabe, S. Hecht, *Adv. Mater.* **2006**, *18*, 1271–1275; d) A. Ajayaghosh, P. Chithra, R. Varghese, *Angew. Chem.* **2007**, *119*, 234–237; *Angew. Chem. Int. Ed.* **2007**, *46*, 230–233; e) P. Chithra, R. Varghese, K. P. Divya, A. Ajayaghosh, *Chem. Asian J.* **2008**, *3*, 1365–1373.

[8] For selected recent reviews, see: a) J. H. Davis, Jr., *Chem. Lett.* **2004**, *33*, 1072–1077; b) Z. Fei, T. J. Geldbach, D. Zhao, P. J. Dyson, *Chem. Eur. J.* **2006**, *12*, 2122–2130; c) A. D. Headley, B. Ni, *Aldrichimica Acta* **2007**, *40*, 107–117; d) P. Domínguez de María, *Angew. Chem.* **2008**, *120*, 7066–7075; *Angew. Chem. Int. Ed.* **2008**, *47*, 6960–6968; e) S. Luo, L. Zhang, J.-P. Cheng, *Chem. Asian J.* **2009**, *4*, 1184–1195; f) Y. Gu, G. Li, *Adv. Synth. Catal.* **2009**, *351*, 817–847.

[9] For selected recent examples, see: a) M. Yoshio, T. Kagata, K. Hoshino, T. Mukai, H. Ohno, T. Kato, *J. Am. Chem. Soc.* **2006**, *128*, 5570–5577; b) Y. Zhang, Y. Shen, J. Yuan, D. Han, Z. Wang, Q. Zhang, L. Niu, *Angew. Chem.* **2006**, *118*, 5999–6002; *Angew. Chem. Int. Ed.* **2006**, *45*, 5867–5870; c) P. H. J. Kouwer, T. M. Swager, *J. Am. Chem. Soc.* **2007**, *129*, 14042–14052; d) Y. Xie, Z. Zhang, T. Jiang, J. He, B. Han, T. Wu, K. Ding, *Angew. Chem.* **2007**, *119*, 7393–7396; *Angew. Chem. Int. Ed.* **2007**, *46*, 7255–7258; e) Z. Zhang, Y. Xie, W. Li, S. Hu, J. Song, T. Jiang, B. Han, *Angew. Chem.* **2008**, *120*, 1143–1145; *Angew. Chem. Int. Ed.* **2008**, *47*, 1127–1129; f) H. Shimura, M. Yoshio, K. Hoshino, T. Mukai, H. Ohno, T. Kato, *J. Am. Chem. Soc.* **2008**, *130*, 1759–1765; g) S. Yazaki, M. Funahashi, T. Kato, *J. Am. Chem. Soc.* **2008**, *130*, 13206–13207; h) K. E. Gutowski, E. J. Maginn, *J. Am. Chem. Soc.* **2008**, *130*, 14690–14704; i) Y. Leng, J. Wang, D. Zhu, X. Ren, H. Ge, L. Shen, *Angew. Chem.* **2009**, *121*, 174–177; *Angew. Chem. Int. Ed.* **2009**, *48*, 168–171; j) J. S. Lee, X. Wang, H. Luo, G. A. Baker, S. Dai, *J. Am. Chem. Soc.* **2009**, *131*, 4596–4597; k) W. Dobbs, B. Heinrich, C. Bourgogne, B. Donnio, E. Terazzi, M.-E. Bonnet, F. Stock, P. Erbacher, A.-L. Bolcato-Bellemin, L. Douce, *J. Am. Chem. Soc.* **2009**, *131*, 13338–13346; l) M. A. Alam, J. Motoyanagi, Y. Yamamoto, T. Fukushima, J. Kim, K. Kato, M. Takata, A. Saeki, S. Seki, S. Tagawa, T. Aida, *J. Am. Chem. Soc.* **2009**, *131*, 17722–17723.

[10] a) W. Chen, Y. Zhang, L. Zhu, J. Lan, R. Xie, J. You, *J. Am. Chem. Soc.* **2007**, *129*, 13879–13886; b) Y. Zhang, X. Chen, J. Lan, J. You, L. Chen, *Chem. Biol. Drug Des.* **2009**, *74*, 282–288.

[11] S. Yagi, Y. Hyodo, M. Hirose, H. Nakazumi, Y. Sakurai, A. S. Yagi, Y. Hyodo, M. Hirose, H. Nakazumi, Y. Sakurai, A. Ajayaghosh, *Org. Lett.* **2007**, *9*, 1999–2002.

[12] a) B. P. Espósito, S. Epsztejn, W. Breuer, Z. I. Cabantchik, *Anal. Biochem.* **2002**, *304*, 1–18; b) R. M. Berne, M. N. Levy, *Physiology*, 3rd ed., Mosby Year Book, St. Louis, **1988**, pp. 705–706.

[13] Selected examples, see: a) J. L. Bricks, A. Kovalchuk, C. Trieflinger, M. Nofz, M. Büschel, A. I. Tolmachev, J. Daub, K. Rurack, *J. Am. Chem. Soc.* **2005**, *127*, 13522–13529; b) T. Gupta, M. E. Van der Boom, *J. Am. Chem. Soc.* **2007**, *129*, 12296–12303.

[14] a) W. Breuer, S. Epsztejn, Z. I. Cabantchik, *J. Biol. Chem.* **1995**, *270*, 24209–24215; b) L.-J. Fan, W. E. Jones, Jr., *J. Am. Chem. Soc.* **2006**, *128*, 6784–6785.

[15] J. V. Ros-Lis, R. Martínez-Máñez, F. Sancenón, J. Soto, M. Spieles, K. Rurack, *Chem. Eur. J.* **2008**, *14*, 10101–10114.

[16] a) J. V. Ros-Lis, M. D. Marcos, R. Martínez-Máñez, K. Rurack, J. Soto, *Angew. Chem.* **2005**, *117*, 4479–4482; *Angew. Chem. Int. Ed.* **2005**, *44*, 4405–4407; b) H. S. Hewage, E. V. Anslyn, *J. Am. Chem. Soc.* **2009**, *131*, 13099–13106.

[17] a) E. W. Miller, C. J. Chang, *Curr. Opin. Chem. Biol.* **2007**, *11*, 620–625; b) S. Kenmoku, Y. Urano, H. Kojima, T. Nagano, *J. Am. Chem. Soc.* **2007**, *129*, 7313–7318; c) Y. Koide, Y. Urano, S. Kenmoku, H. Kojima, T. Nagano, *J. Am. Chem. Soc.* **2007**, *129*, 10324–10325; d) B. C. Dickinson, C. J. Chang, *J. Am. Chem. Soc.* **2008**, *130*, 9638–9639.

[18] L. Beverina, M. Crippa, P. Salice, R. Ruffo, C. Ferrante, I. Fortunati, R. Signorini, C. M. Mari, R. Bozio, A. Facchetti, G. A. Pagani, *Chem. Mater.* **2008**, *20*, 3242–3244.

[19] E. A. Jaffe, R. L. Nachman, C. G. Becker, C. R. Minick, *J. Clin. Invest.* **1973**, *52*, 2745–2756.

Received: December 21, 2009
Published online: March 26, 2010

